Supported base metal catalysts for the preferential oxidation of carbon monoxide in the presence of hydrogen (PROX)

Fernando Marino, Claude Descorme, Daniel Duprez

Supported base metal catalysts for the preferential oxidation of carbon monoxide in the presence of excess hydrogen (PROX)

Fernando Mariño[a,b,*], Claude Descorme[a,c], Daniel Duprez[a]

[a]*LACCO-UMR 6503, CNRS-Université de Poitiers, 40 Avenue du Recteur Pineau, F-86022 Poitiers Cedex, France*
[b]*Laboratorio de Procesos Catalíticos, DIQ-FIUBA, Universidad de Buenos Aires, Pabellón de Industrias, Ciudad Universitaria, 1428 Buenos Aires, Argentina*
[c]*Institut de Recherches sur la Catalyse (IRC), CNRS, 2 Avenue Albert Einstein, F-69626 Villeurbanne Cedex, France*

Supported base metal catalysts were tested for the preferential oxidation of CO (CO PROX). The catalysts we investigated covered a wide range of transition metals (Co, Cr, Cu, Ni, Zn) supported on oxides with very different acidic, basic and redox properties (MgO, La_2O_3, SiO_2–Al_2O_3, CeO_2, $Ce_{0.63}Zr_{0.37}O_2$). The influence of the metal loading (Cu), the support properties (acidity, basicity, redox, surface area) and the reaction conditions (reaction temperature, feed composition) on the catalyst activity and selectivity was evaluated. The activity of ceria and ceria–zirconia supported copper catalysts was comparable to the performances of noble metal samples classically used for the PROX reaction. In addition, Cu–CeO_2 catalysts showed a practically constant and high selectivity towards CO oxidation in the temperature range of 50–150 °C. Due to the strong synergetic effect between copper and ceria, only a small amount of copper (0.3 wt.%) was necessary to get an active catalyst. The best catalytic performances were obtained for the samples containing 1–3 wt.% copper. The presence of small copper particles in close interaction with the ceria support was shown to be responsible for the enhanced activity. Except for the hydrogen oxidation, no parallel reactions (CO or CO_2 methanation reactions, coking, RWGS) could be detected over these catalysts. Classically, an increase of the oxygen excess led to an increased CO conversion with a simultaneous loss of selectivity towards CO_2. Finally, the presence of CO_2 in the feed negatively affected the catalytic activity. This effect was attributed to the adsorption of CO_2 on the copper sites, probably as CO.

Keywords: Preferential oxidation of CO; PROX; Base metals; Copper; Ceria; Supported catalysts; Redox; Oxygen mobility; Hydrogen purification; Fuel cells

1. Introduction

In the past years, low-temperature proton-exchange membrane fuel cells (PEMFC) have largely been studied and developed, especially for vehicle applications. Although pure hydrogen is the ideal fuel for PEMFC, in order to avoid the problems related with H_2 distribution and storage, a reasonable alternative is the on-board production of hydrogen.

The hydrogen produced via the steam reforming or the partial oxidation of hydrocarbons or renewable fuels generally contains 0.5–2.0 vol.% CO. Unfortunately, PEMFC electrodes are extremely sensitive to even low levels of carbon monoxide (50 ppm). As a consequence, the hydrogen fed to the anode should be almost free of CO.

Out of the methods available for removing carbon monoxide from hydrogen-rich streams, the preferential oxidation of CO (CO PROX) seems to be the simplest and the least expensive one.

The PROX reaction has been extensively studied over supported noble metal (Pt, Rh, Ru, Pd, Ir) catalysts [1–4]. In particular, some authors [5–7] have demonstrated that gold, which was considered to be inert for catalytic applications, is indeed a good catalyst for the low-temperature selective CO oxidation.

* Corresponding author. Tel.: +54 114 576 3240; fax: +54 114 576 3241.
E-mail address: fernando@di.fcen.uba.ar (F. Mariño).

However, the high cost of precious metals has encouraged researchers around the world to look for alternative catalysts. Ceria or ceria–zirconia-supported transition metal catalysts (Cu, Co, Ni) have been reported as highly active for the CO oxidation in the absence of hydrogen [8–10]. The CuO–CeO_2 catalyst has been found to be highly active and exceptionally selective for the preferential oxidation of CO [10–15].

Fluorite-type oxides (CeO_2, CeO_2–ZrO_2) were shown to be some very interesting supports for the total oxidation reactions. In fact, in the case of CeO_2 and CeO_2-based supports the redox cycle Ce(III)–Ce(IV) is easy and the oxygen mobility in the crystallographic structure is very much facilitated. As a result, such oxides are able to reversibly ''absorb'' oxygen [16,17]. The high activity of the above-mentioned CuO–CeO_2 catalyst, comparable with or even superior to the performances of the costly precious metal catalysts, was attributed to the strong interaction between the copper nanoparticles and the ceria support [18–20]. It was proposed that well-dispersed CuO on CeO_2, which is reducible at lower temperatures with respect to bulk CuO, could easily adsorb CO. As a consequence, this catalyst exhibited a high activity/selectivity for the low-temperature CO oxidation [21–23]. Additionally, it was demonstrated that the redox processes undergone upon the CO oxidation involved the reduction and the oxidation of both the copper and the ceria phases [24–27]. It was also postulated that the presence of copper enhances the redox behavior, the oxygen storage capacity and the thermal stability of ceria [28,29].

In the present work we have explored the catalytic performances of several ceria and ceria–zirconia supported base metal (Co, Cr, Cu, Ni, Zn) catalysts. In addition, other oxides with different acidic and basic properties (SiO_2–Al_2O_3, La_2O_3, MgO) were used as supports. This study was carried out because a correlation could be found between the basicity of the support and the oxygen surface migration kinetics in the case of noble metal catalysts [4,30,31]. In this work, the effect of such supports was only examined for the copper catalysts. In fact, the final goal of this research was to identify the important functionalities of the catalyst, both the metal and the support, in order to be able to optimize the catalytic formulation. For that, one has to know whether acidic, basic or reducible supports should be preferred and what are the requirements for the metallic phase.

2. Experimental

Base metal (Co, Cr, Cu, Ni, Zn) catalysts supported on various oxides ($Ce_{0.63}Zr_{0.37}O_2$, CeO_2, SiO_2–Al_2O_3, La_2O_3, MgO) were evaluated in the preferential oxidation of CO. The suppliers for the different supports are listed in Table 1.

The catalysts were prepared by simple impregnation of the supports with the corresponding aqueous solutions of the metal precursor salts ($Co(NO_3)_2{\cdot}6H_2O$, $Cr(NO_3)_3{\cdot}9H_2O$, $Cu(NO_3)_2{\cdot}3H_2O$, $Ni(NO_3)_2{\cdot}6H_2O$ and $Zn(C_2H_3O_2)_2{\cdot}2H_2O$). The catalysts were subsequently dried at 120 °C for 24 h and finally calcined for 4 h at 450 °C under flowing air (30 mL min^{-1}).

Table 1
BET surface area and suppliers of the bare oxide supports

Support	Supplier	S_{BET} ($m^2\,g^{-1}$)
$Ce_{0.63}Zr_{0.37}O_2$	Rhodia catalysis and electronics	43
CeO_2 ^{lsa}	Rhodia catalysis and electronics	25
CeO_2 ^{hsa}	Rhodia catalysis and electronics	160
MgO	Ube material industries	66
La_2O_3	Home-synthesized	≈2
SiO_2–Al_2O_3	Akzo chemie	525

Surface areas (S_{BET}) of the bare supports, measured by N_2 adsorption at −196 °C using the single point method and a Micromeretics Flowsorb II apparatus, are presented in Table 1.

As it will be discussed later, the dispersion of the copper phase over ceria or ceria–zirconia is a key parameter that may determine the performances of these catalysts. Traditional methods to evaluate the copper dispersion involve the selective chemisorption of N_2O molecules over the surface copper atoms [32–34]. However, when this method was applied to the pre-reduced CuO–CeO_2 catalysts, the amount of N_2 released after the N_2O chemisorption was higher than the total copper loading of the catalyst. The excess N_2 was attributed to the reaction between N_2O and the hydrogen adsorbed on the ceria surface after the reduction pre-treatment. Therefore, we could not determine the copper surface area and the copper dispersion since the presence of ceria perturbed the measurements.

The structure of the ceria-supported copper catalysts was characterized by XRD using a Siemens D5005 diffractometer. Crystalline phases were identified by comparison with ICDD files. The average crystallite sizes were derived from the Scherrer equation.

Catalytic tests were carried out in an atmospheric glass fixed bed reactor placed in an electrical oven. In a typical run, the mass of catalyst was fixed at 100 mg. Because of the small size of the catalyst bed (8 mm in diameter and 4 mm in height), it was assumed that there was no significant temperature profile in the bed. In general, the reaction mixture consisted in 70 vol.% H_2, 2 vol.% CO, 1–4 vol.% O_2 (oxygen excess, $\lambda = 2p_{O_2}/p_{CO}$, varies from 1 to 4) and N_2 as a balance. In some experiments, up to 15 vol.% of CO_2 were also added to the feed. The total inlet gas flow rate was fixed at 100 N mL min^{-1}. Analytical grade cylinders (Alphagas-1 from Air Liquide) of hydrogen, nitrogen, CO, CO_2 and O_2 were used. Before each experiment the catalyst was pre-conditioned in situ under 100 N mL min^{-1} of flowing air at 300 °C for 30 min. During the reaction, the reactor temperature was progressively ramped, using a temperature controller, from 50 to 300 °C at a rate of 1 °C min^{-1}. After that, the reactor was cooled down to 50 °C. Similar activity and selectivity values were obtained

at a given temperature whatever the temperature was evolving upwards or downwards. In addition, a restricted number of steady-state experiments was carried out at a few fixed temperatures. The goal was to verify whether the conversions and selectivities measured upon temperature programmed experiments would be the same as the steady-state values.

At the reactor outlet, the analysis of the non-converted reactants (CO, H_2, O_2) and the gaseous products (CO_2, CH_4) was performed using a combination of two gas chromatographs. One chromatograph was equipped with a CTR column and helium was used as the carrier gas while the other chromatograph was equipped with a 5 Å molecular sieve filled column and nitrogen was used as the carrier gas. The second one was only used to determine the H_2 concentration in the outlet gases. In both cases, TCD detectors were used. Additionally, when high CO conversions were obtained, the concentration of carbon monoxide was determined with a specific infrared spectrometer (COSMA Beryl 100).The oxygen and the carbon monoxide conversions were based on the oxygen and the carbon monoxide consumption, respectively:

$$x_{O_2} = \frac{F^{in}_{O_2} - F^{out}_{O_2}}{F^{in}_{O_2}}, \qquad x_{CO} = \frac{F^{in}_{CO} - F^{out}_{CO}}{F^{in}_{CO}}$$

where F_i^{in} and F_i^{out} are the inlet and outlet molar flows of gas i, respectively.

The selectivity to CO_2 (desired reaction) was calculated as:

$$S_{CO_2} = \frac{F^{out}_{CO_2}}{2(F^{in}_{O_2} - F^{out}_{O_2})}$$

Nevertheless, in the experiments where CO_2 was also added to the feed, the selectivity towards CO_2 was alternatively calculated as:

$$S_{CO_2} = \frac{1}{2}\left(\frac{F^{in}_{CO} - F^{out}_{CO}}{F^{in}_{O_2} - F^{out}_{O_2}}\right)$$

It should be noted that this formula was used in experiments with Cu–CeO_2 catalysts. As it will be shown in this work, methanation reactions do not occur over such a catalyst. As a result, CO is exclusively converted to CO_2.

3. Results

3.1. Catalyst formulation

The evolutions as a function of temperature of the CO and O_2 conversions and the CO_2 selectivity obtained over M–$Ce_{0.63}Zr_{0.37}O_2$ catalysts (M = Co, Cr, Cu, Ni, Zn) are presented on Fig. 1. The metal content for all the catalysts was fixed at 1 wt.%.

The copper catalyst showed the best behavior, with a maximum CO conversion at temperatures around 150 °C

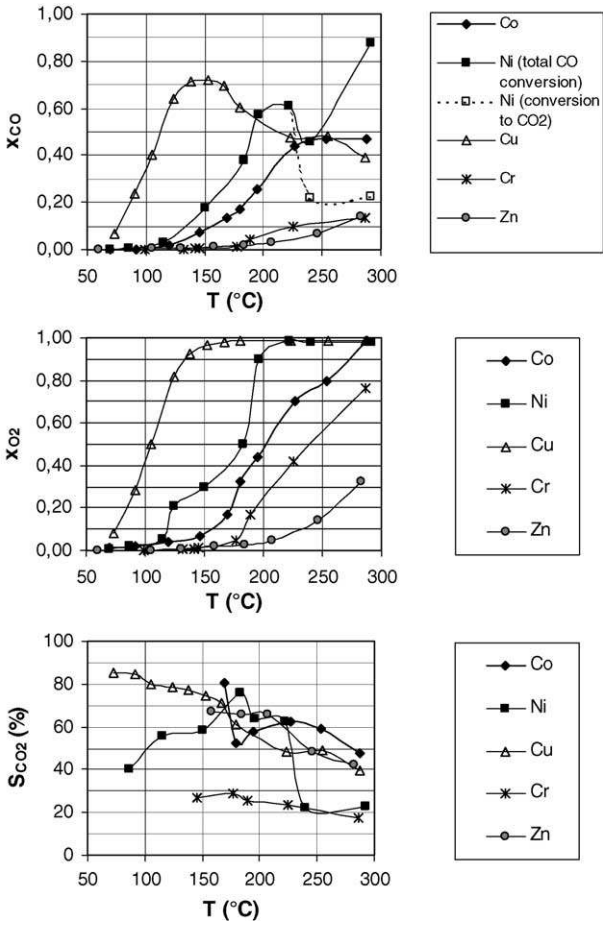

Fig. 1. CO preferential oxidation over 1% M/$Ce_{0.63}Zr_{0.37}O_2$ (M = Co, Cr, Cu, Ni, Zn). Evolution of the CO conversion, the O_2 conversion and the CO_2 selectivity as a function of the reaction temperature. (Mass of catalyst = 100 mg; total flow = 100 N mL min^{-1}; feed composition: 70% H_2, 27% N_2, 2% CO, 1% O_2 (λ = 1)).

and a complete oxygen conversion for temperatures higher than 175 °C. Oxygen and CO conversions behave in a similar way in the temperature range between 50 and 150 °C, resulting in a practically constant selectivity. However, above 175 °C the hydrogen oxidation reaction became much more rapid and both the CO conversion and the CO_2 selectivity decreased.

Looking at the nickel catalyst, although some good results were obtained at low temperature, high activities in the CO methanation reaction were also evidenced for temperatures higher than 220 °C.

Cobalt was not very active at low temperature, however, the CO conversion achieved above 200 °C was similar to the one obtained over the copper catalyst. Finally, the other two metals (Cr, Zn) were almost inactive for the CO preferential oxidation.

In conclusion, the best results were obtained with copper. As a result, the other metals were discarded and only copper catalysts will be further analyzed. The effect of the support was examined through the evaluation of a series of supported 3 wt.% copper catalysts (Fig. 2). The oxides used as supports

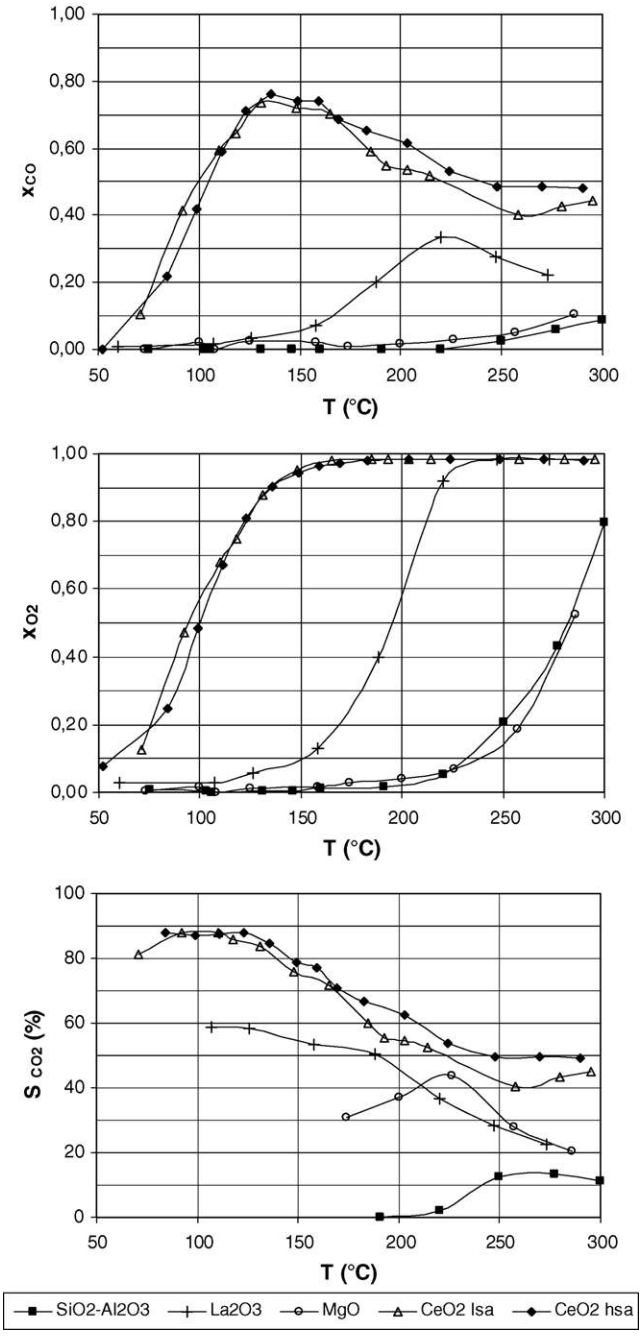

Fig. 2. CO preferential oxidation over supported 3 wt.% Cu catalysts. Evolution of the CO conversion, the O_2 conversion and the CO_2 selectivity as a function of the reaction temperature. (Mass of catalyst = 100 mg; total flow = 100 N mL min^{-1}; feed composition: 70% H_2, 27% N_2, 2% CO, 1% O_2 ($\lambda = 1$)].

were CeO_2, SiO_2–Al_2O_3, La_2O_3 and MgO. The idea was to check whether the support should better be acidic, basic and/or reducible.

Very poor CO conversions were obtained with both acidic only (SiO_2–Al_2O_3) and basic only (La_2O_3, MgO) supports. On the contrary, a high CO removal level was achieved with CeO_2. Even though ceria is both a basic and a reducible support, it appears from the results obtained on the basic only supports that the redox properties of the support play a major role in promoting the catalyst performances.

The effect of the surface area of the support was also examined (Fig. 2). Two ceria-supported copper catalysts were compared. One catalyst was prepared on a high surface area ceria (CeO_2^{hsa}, 160 $m^2\ g^{-1}$) and the other copper catalyst was supported on a low surface area ceria (CeO_2^{lsa}, 25 $m^2\ g^{-1}$). As it can be seen, the surface area of the ceria support does not significantly affect the catalyst activity and selectivity.

If one assumes that the copper dispersion is the same for both catalysts (3 wt.% Cu–CeO_2^{hsa} and 3 wt.% Cu–CeO_2^{lsa}), the absence of any effect of the surface area could possibly indicate that the reaction takes place at the metal–support interface. The enhanced activity of the ceria-supported copper catalysts could originate for the very specific sites created at the copper nanoparticle perimeter. This hypothesis could be verified by varying the copper dispersion while the copper loading and the support surface area are kept constant. However, such a study enforces the development of a new method for the determination of the copper surface area in a Cu–CeO_2 catalyst.

From the above results, Cu–CeO_2 was found to be the best formulation. This ''optimized'' formulation will be the only one studied in the next sections.

3.2. Effect of the copper content

Fig. 3 shows the evolutions of the CO and O_2 conversions and the CO_2 selectivity as a function of temperature for a series of Cu–CeO_2^{lsa} catalysts, with a nominal metal loading ranging from 0.3 to 10 wt.%. In the same figure, the performances of the bare support was added for comparison purposes.

It can be observed that all the catalysts exhibit much higher activities than the ceria support alone. Among the whole copper loading domain we looked at, the best results were found for the catalysts containing 1–3 wt.% copper.

Fig. 4 shows the XRD diffraction patterns for four of these catalysts. For all of them, the fluorite-type cubic structure of the ceria support is maintained (ICDD file 34-0394). In addition, a CuO crystalline phase (tenorite, ICDD file 45-0937) was detected for the catalysts containing more than 3 wt.% of copper. The mean diameter of the copper oxide crystallites, calculated from the X-ray line broadening according to the Scherrer's equation, was 34 nm for 5% Cu–CeO_2^{lsa} and 42 nm for 10% Cu–CeO_2^{lsa}. Such a determination was not possible for the other two samples.

Liu and Flytzani-Stephanopoulos [18] found some similar values (29 nm) for a series of $Cu_x[Ce(La)]_{(1-x)}O_2$ catalysts prepared by co-impregnation.

3.3. Side reactions

As it was mentioned earlier in the text, the methanation reaction could take place on some PROX catalysts and

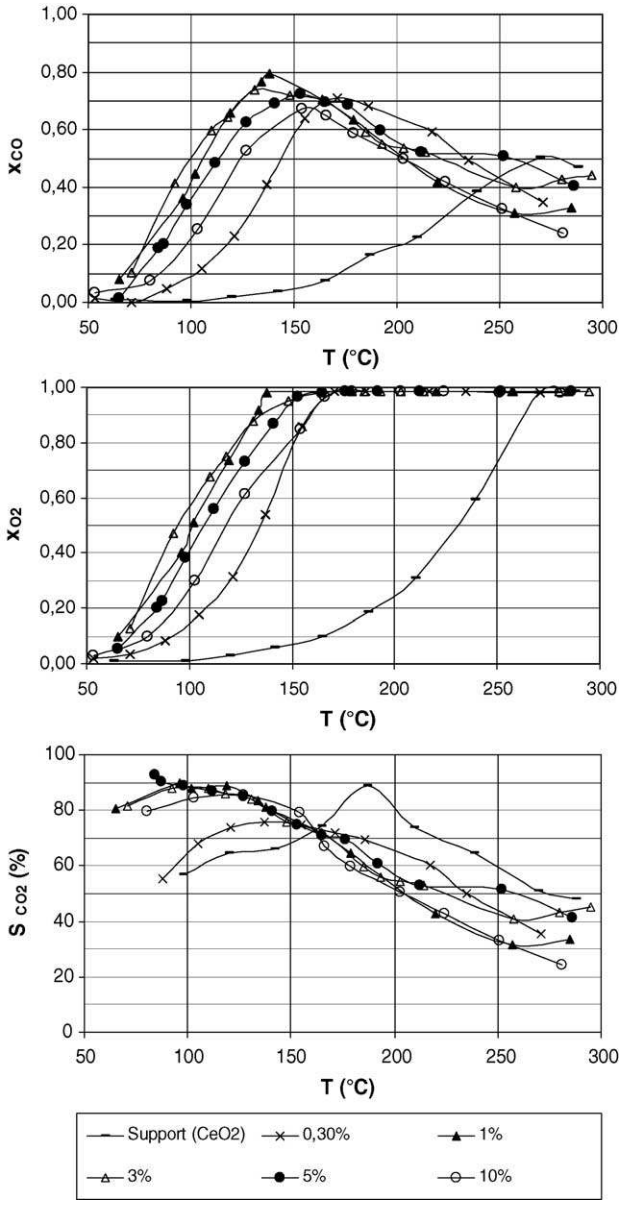

Fig. 3. CO preferential oxidation over a series of Cu–CeO_2[lsa] catalysts (nominal Cu loading ranking between 0.3 and 10 wt.%) and over the bare ceria support. Evolution of the CO conversion, the O_2 conversion and the CO_2 selectivity as a function of the reaction temperature. (Mass of catalyst = 100 mg; total flow = 100 N mL min^{-1}; feed composition: 70% H_2, 27% N_2, 2% CO, 1% O_2 ($\lambda = 1$)).

consequently reduce the amount of hydrogen produced by the overall process. Nevertheless, for such Cu–CeO_2 catalysts, not even traces of methane were detected at the reactor outlet at any temperature analyzed. Then, both the CO and CO_2 methanation can be disregarded.

In addition, the carbon balance showed that the CO_2 production is in good agreement with the CO consumption. For this reason, coking over such catalysts could also be disregarded.

Furthermore, the reverse water gas shift (RWGS) reaction would form CO from CO_2 and reduce the overall CO

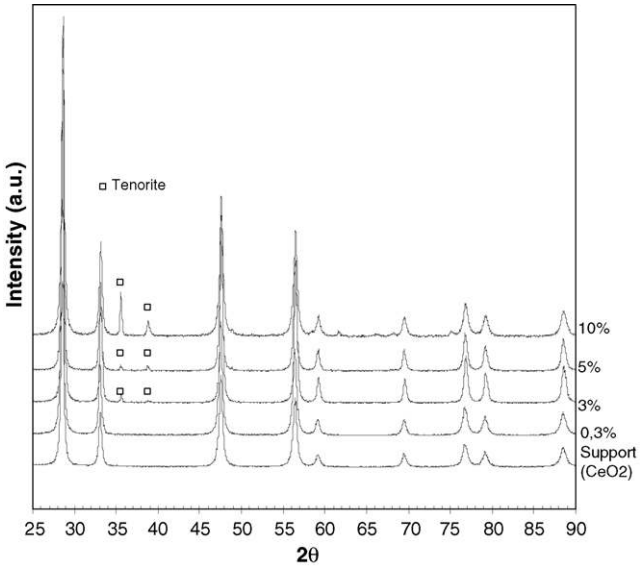

Fig. 4. XRD patterns of a series of Cu–CeO_2[lsa] catalysts (nominal Cu loading ranking between 0.3 and 10 wt.%) and the bare ceria support.

conversion that might be attained in the PROX reactor. To evaluate whether the RWGS reaction takes place over the Cu–CeO_2[hsa] catalysts, we performed some additional experiences where a CO_2–H_2 mixture (25% CO_2, 25% H_2 and 50% N_2) was fed to the reactor. The CO concentration at the reactor outlet is shown in Fig. 5 as a function of the reactor temperature. As it can be observed, the catalyst is not active for the RWGS for temperatures lower than 200 °C. Above 200 °C, a mild concentration in CO can be detected in the reaction products. The maximum conversion to CO, reached at about 300 °C, was only 1.1%. This last value clearly confirms that the reaction mixture is not thermodynamically equilibrated even at 300 °C. In our case, the reaction is under kinetic control. While CuO–CeO_2 samples have been described as active catalysts for the WGSR [35] our results have shown that the RWGS reaction on these catalysts could be disregarded. To explain this discrepancy, a self-poisoning of the active sites by the adsorbed CO_2 species could be proposed.

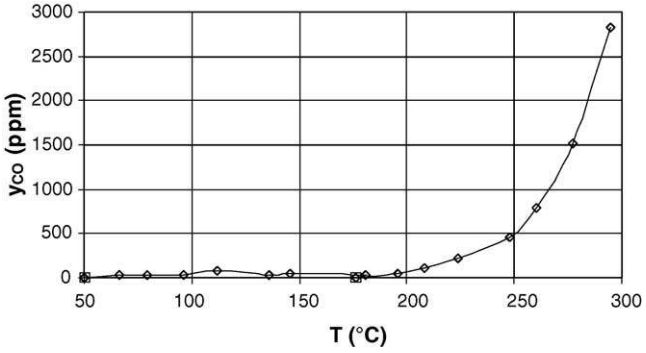

Fig. 5. RWGS reaction over a 3% Cu–CeO_2[hsa] catalyst. Evolution of the outlet CO molar fraction as a function of the reaction temperature. (Mass of catalyst = 100 mg; total flow = 100 N mL min^{-1}; feed composition: 25% CO_2, 25% H_2, 50% N_2].

3.4. Effect of the feed composition

First of all, we studied the effect of the oxygen excess (λ). The evolutions of the CO and O_2 conversions and the CO_2 selectivity obtained upon reaction over 3% Cu–CeO_2^{hsa} at different λ values are shown on Fig. 6.

The CO conversion increases as the oxygen partial pressure in the feed increases. However, a parallel decrease of the CO_2 selectivity is observed. This observation indicates

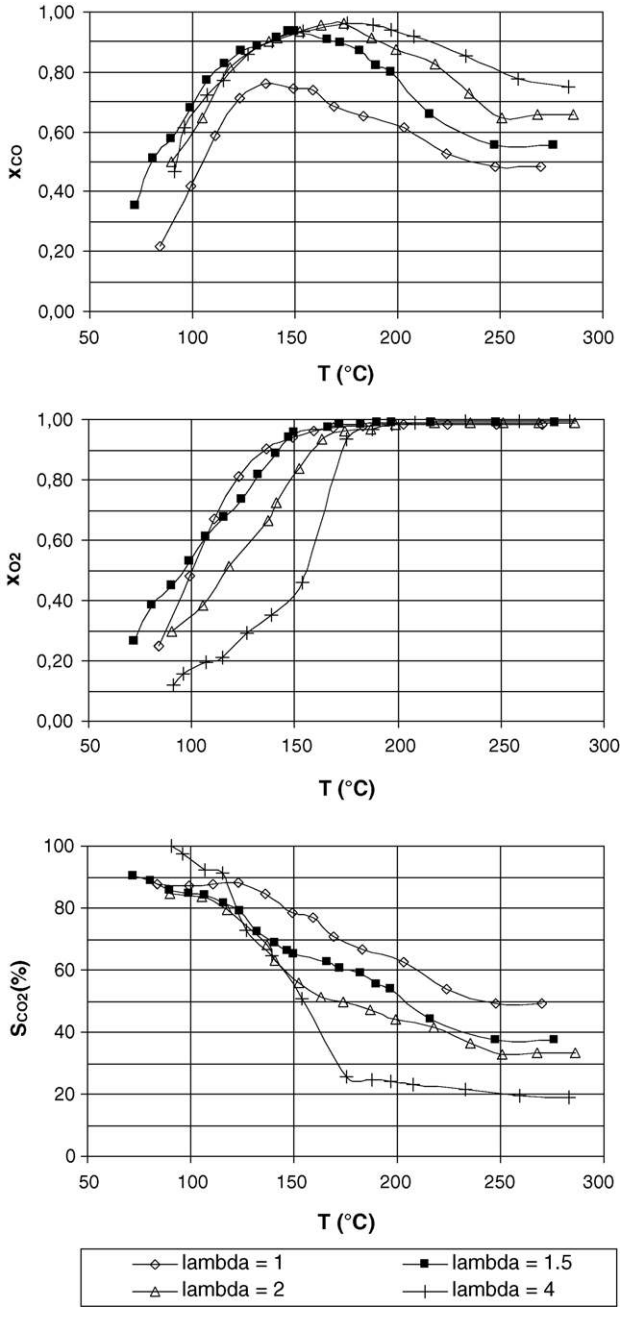

Fig. 6. CO preferential oxidation over a 3% Cu–CeO_2^{hsa} catalyst: effect of the oxygen excess (λ). Evolution of the CO conversion, the O_2 conversion and the CO_2 selectivity as a function of the reaction temperature. (Mass of catalyst = 100 mg; total flow = 100 N mL min^{-1}; feed composition: 70% H_2, 2% CO, 1–4% O_2 (λ = 1–4) and N_2 (balance)).

Table 2
Effect of the presence of CO_2 in the feed

y_{CO_2} (%)	T_{50} (°C)
0	101
5	123
15	141

Catalyst: 3 wt.% Cu–CeO_2^{lsa}; feed composition: $y_{H_2} = 70\%$; $y_{CO} = 2\%$; $y_{O_2} = 1\%$ (λ = 1).

that the 3% Cu–CeO_2^{hsa} catalyst is intrinsically selective towards the oxidation of CO to CO_2. In fact, the hydrogen oxidation reaction is only favored in the presence of large excess of oxygen. In fact, one must keep in mind that ceria can act as an oxygen buffer. As a result, the oxygen concentration over the catalyst would virtually be constant up to a certain oxygen inlet concentration when the maximum oxygen storage capacity (OSC) of ceria is exceeded. Once again, the parallel between the enhanced OSC of ceria in the presence of copper and the optimized catalytic performances of such a formulation should be underlined.

Furthermore, the presence of CO_2 in the reaction feed, up to 15 vol.%, was also examined. Table 2 shows the temperature required to obtain 50% conversion of CO (T_{50}) in the PROX reactor.

As it can be deduced from this table, the presence of CO_2 in the feed induces a loss in the catalytic performances. This effect is more and more pronounced as the CO_2 partial pressure in the feed increases and could tentatively be explained by the adsorption of CO_2 on the ceria surface as carbonates. Such carbonate species could block the oxygen mobility on the ceria surface and lower the activity. If this hypothesis is verified the activity should decrease continuously up to the point when the ceria surface is completely saturated with adsorbed carbonate species. This saturation was not observed in our experiments up to 15 vol.% CO_2.

4. Discussion

In this work a large series of supported base metal catalysts were examined as potential substitutes for the classical noble metal based PROX catalysts. Our results have shown that only the ceria- and ceria–zirconia-supported copper catalysts could be considered as comparable in performances with the noble metal samples for the oxidation of carbon monoxide in the presence of large quantities of hydrogen. Moreover, these Cu–CeO_2 catalysts exhibited a practically constant and high selectivity towards CO oxidation in the temperature range of 50–150 °C. Consequently, ceria-supported copper catalysts offer a wider temperature window for the operation of the PROX reactor and the PEM fuel cell compared to costly noble metal based catalysts. It must be remembered at this point that the selectivity towards the CO oxidation on the noble metal catalysts, such as Pt–Al_2O_3, continuously decreases as the

temperature increases for $T > 90$ °C [4]. Recently, Kandoi et al. [15] using some density functional theory calculations and micro-kinetic models, explained that Cu is more selective than Pt due to: (i) differences in the CO and H_2 coverages over the different metal surfaces; and (ii) differences in the rate constants for the two competitive oxidation reactions (CO versus H_2).

The supported CuO–CeO_2 catalyst under study has demonstrated similar catalytic performances compared to the early studied CuO–CeO_2 mixed oxide catalysts prepared via the urea-nitrate combustion method [11], the co-precipitation method [20,36] or the sol–gel method [37,38]. All these catalysts exhibit a high CO oxidation activity and a high selectivity towards CO_2 at low temperature. At higher temperature, the H_2 oxidation reaction levels up and a maximum CO conversion is observed as a function of temperature.

The CO oxidation over the metal is thought to follow a competitive Langmuir–Hinshelwood mechanism: CO and O_2 adsorb on the same sites. However, some Authors also proposed the Eley–Rideal mechanism: gas-phase CO directly reacts with adsorbed oxygen.

The mechanism for the CO oxidation over the metals supported on reducible metal oxides is totally different. In fact, the reaction is thought to occur in two steps according to the mechanism suggested by Mars and van Krevelen in 1954 [39]. First, the CO adsorbed on the metal sites is oxidized by the lattice oxygen atoms from the active metal oxide. As a result, an oxygen vacancy is created and the neighboring metal atom is reduced. In a second step, the surface metal atom is re-oxidized by the gas phase oxygen. In such a scheme, H_2 and CO compete for the same adsorption site and the hydrogen oxidation is suppressed or at least reduced due to the stronger CO adsorption. Furthermore, active supports, such as ceria-based supports, were also shown to store hydrogen at low temperature [40]. Such a capacity would potentially reduce the hydrogen partial pressure above the catalyst, lower the hydrogen coverage and enhanced the catalyst selectivity.

Since the oxidation over such catalysts takes place via a redox mechanism, the ability of the metal oxide to undergo redox cycles is crucial for the activity in the PROX reaction. The key role of the support might clearly be observed on Fig. 2. The activity of the supported copper catalysts was practically negligible, except for the ceria-based samples.

Furthermore, as mentioned in Section 1, the oxygen activation was found to proceed more readily on basic oxide supported noble metal catalysts than on acidic oxide ones [4]. However, the only acidity and/or the basicity of the different oxides used as supports did not significantly affect the performances of the copper catalysts tested. Nevertheless, the ceria or ceria–zirconia-supported copper catalysts, independently of the surface area of the support, were shown to be very active for the CO selective oxidation. In that case one should note that ceria-based oxides are basic and that the oxygen is very mobile on such supports.

Concerning the copper content of the Cu–CeO_2 catalysts presented in this work, the results have shown that:

- Only small amounts of copper are needed to obtain an active catalyst, as it can be concluded if we compare the catalytic behavior of the bare CeO_2 and the 0.3% Cu–CeO_2 sample.
- The samples containing 1 and 3 wt.% Cu were the most active and selective catalysts.
- Copper in excess forms bulk CuO which is practically inactive for the PROX reaction. Bulk CuO was detectable in our XRD diffractograms for the catalysts containing more than 3 wt.% Cu. Dong et al. [41] have stated that the dispersion capacity of ceria supported copper oxide catalysts is 1.2 mmol of CuO/100 m^2 of CeO_2. Our XRD results are in good agreement with this limit mentioned by Dong et al. In our case, for the CeO_2^{lsa} support (25 m^2 g^{-1}), the limit would be 1.87 wt.% Cu.

In fact, it was already known that:

(i) bulk CeO_2 is practically inactive in the CO oxidation reaction;
(ii) bulk CuO is enable to chemisorb CO [22];
(iii) bulk CuO is active at much higher reaction temperatures than the Cu–CeO_2 catalysts [18].

Furthermore, several works already proposed some theories about the synergism between copper and cerium in the Cu–CeO_2 catalysts. In such models, CO (and H_2) adsorption is supposed to take place on the copper sites while CeO_2 provides the oxygen source. In this way, the oxidation reactions proceed at the metal–support interface. Furthermore, it was also postulated that the presence of CeO_2 increases the dispersion of copper oxide and enhances the redox behavior of the copper ions, and that the presence of copper, in turns, increases the reducibility of ceria [29,42]. Finally, some authors reported that synergetic effects would involve the stabilization by the ceria support of non-stoichiometric metastable copper oxide species formed during the reduction, which species would be highly active for the CO oxidation reaction [43].

In agreement with the above mentioned Mars and van Krevelen mechanism, the high activity of the Cu–CeO_2 or Cu–$Ce_{0.63}Zr_{0.37}O_2$ catalysts observed in our experiments seemed to be determined by the ability of ceria to incorporate oxygen from the gas phase and to transfer it to the active centers. In addition, since the active sites are located at the metal–support interfacial region, the amount of these sites is strongly dependent of the copper particle size. The very finely dispersed copper nanoparticles certainly present in the low metal content samples (copper content between 1 and 3 wt.%), not detectable in our XRD patterns, appeared in fact to be very active for the CO oxidation reaction. These copper nanoparticles would be

Table 3
Optimal CO conversion achieved as a function of the oxygen excess (λ) along with the corresponding CO_2 selectivity and reaction temperature

Oxygen excess (λ)	x^*_{CO} (%)	$S^*_{CO_2}$ (%)	T^* (°C)
1	76.2	84.6	136
1.5	93.4	66.4	147
2	96.0	49.9	174
4	96.2	25.7	175

Catalyst: 3 wt.% Cu–CeO_2[hsa]; feed composition: $y_{H_2} = 70\%$; $y_{CO} = 2\%$; $y_{O_2} = 1{-}4\%$ (λ = 1–4).

present as isolated cationic species more active for the CO oxidation than the H_2 oxidation. Similar observations were already found for Rh–CeO_2 catalysts [44], in which Rh cations were the most active species for the CO oxidation. At higher metal content, the large copper particles detected in the XRD patterns contributed very slightly to the overall activity. Accordingly with the reaction pathways reviewed in the above paragraph, the decrease in the activity and the selectivity of the catalysts observed experimentally in the presence of CO_2 would probably be attributed: (i) to the competitive adsorption of CO_2 on the copper sites; and/or (ii) to the inhibition of the oxygen mobility on the ceria support in the presence of adsorbed CO_2, as carbonates.

Moreover, in most of this work, the PROX reaction was investigated in a simplified way; that is, no water or CO_2 but only the reactants (CO, O_2 and H_2) were fed to the reactor. Even in such a basic research, some parallel reactions (methanation, RWGS, coking) could take place and affect the overall process efficiency. However, it was shown in the case of the Cu–CeO_2 catalysts that none of these parallel reactions occur, except the hydrogen oxidation reaction.

Finally, as shown in Fig. 6, the oxygen excess clearly influences the CO and O_2 conversions and the CO_2 selectivity dependencies on the reaction temperature.

In all cases, the CO conversion continuously increases until the oxygen present in the feed is totally consumed. As λ increases, the complete oxygen conversion is attained at higher temperature and the optimum CO conversion is also shifted towards higher temperatures (see Table 3). As a final consequence, it is shown in Table 3 that the optimal CO conversion is higher for higher λ values. Nevertheless, the selectivity towards the CO oxidation reaction strongly decreases at the same time. An increase in the oxygen excess simultaneously leads to a marked loss in the overall process efficiency. In our case, as it might be seen in Table 3, the effect starts from $\lambda \geq 2$. Consequently, the positive effect of λ on the CO conversion is counterbalanced by the simultaneous loss in selectivity towards the oxidation of CO into CO_2. As a result, the overall process efficiency goes through a maximum as a function of the oxygen excess. Obviously, this optimum λ value depends not only on the catalyst formulation but also on the reaction conditions (space time).

5. Conclusions

The preferential oxidation of carbon monoxide in the presence of large quantities of hydrogen was carried out over different supported base metal catalysts. The catalytic formulations involved several transition metals (Co, Cr, Cu, Ni, Zn) supported on oxides with different acidic, basic and redox properties (MgO, La_2O_3, SiO_2–Al_2O_3, CeO_2, $Ce_{0.63}Zr_{0.37}O_2$). Out of them, the only ceria- and ceria–zirconia-supported copper catalysts appeared to be as active as the costly platinum group catalysts classically used for this reaction. Additionally, copper catalysts were very selective in a wide temperature range of 50–150 °C, suitable for the PEM fuel cell operation.

The optimum copper content in the catalyst was found to be in between 1 and 3 wt.%. The presence of small copper particles interacting with the ceria support was confirmed to be crucial. For higher copper loading, bulk CuO almost inactive for the CO oxidation reaction is formed.

Except for the hydrogen oxidation, no parallel reactions (methanation reactions, coking, RWGS) were detected over such copper catalysts.

Finally, an increase in the oxygen excess (λ) had a positive impact on the CO conversion but, at the same time, the selectivity towards CO_2 decreased. In our case, the best CO removal level was obtained on a 1% Cu–CeO_2[lsa] catalyst at 157 °C and λ = 2. Under such reaction conditions, the CO concentration at the reactor outlet was reduced from 20,000 ppm down to approximately 325 ppm, with a selectivity around 56%.

Acknowledgements

Financial support for Dr. Fernando Mariño's post-doctoral stay in France from the French Ministry of Research and New Technologies is gratefully acknowledged.

References

[1] S. Oh, R. Sinkevitch, J. Catal. 142 (1993) 254.
[2] I. Son, M. Shamsuzzoha, M. Lane, J. Catal. 210 (2002) 460.
[3] P. Snytnikov, V. Sobyanin, V. Belyaev, P. Tsyrulnikov, N. Shitova, D. Shlyapin, Appl. Catal. A: Gen. 239 (2003) 149.
[4] F. Mariño, C. Descorme, D. Duprez, Appl. Catal. B: Environ. 54 (2004) 59.
[5] M. Haruta, Catal. Today 36 (1997) 153.
[6] M. Schubert, A. Venugopal, M. Kahlich, V. Plzak, R. Behm, J. Catal. 222 (2004) 32.
[7] C. Costello, J. Yang, H. Law, Y. Wang, J. Lin, L. Marks, M. Kung, H. Kung, Appl. Catal. A: Gen. 243 (2003) 15.
[8] W. Liu, A. Sarofin, M. Flytzani-Stephanopoulos, Appl. Catal. B: Environ. 4 (1994) 167.
[9] T. Huang, T. Yu, Appl. Catal. 72 (1991) 275.
[10] S. Zhang, W. Huang, X. Qiu, B. Li, X. Zheng, S. Wu, Catal. Lett. 80 (1/2) (2002) 41.

[11] G. Avgouropoulos, T. Ioannides, Appl. Catal. A: Gen. 244 (2003) 155.
[12] J. Wang, W. Shih, T. Huang, Appl. Catal. A: Gen. 203 (2000) 191.
[13] D. Kim, J. Cha, Catal. Lett. 86 (1–3) (2003) 107.
[14] J. Wang, D. Tsai, T. Huang, J. Catal. 208 (2002) 370.
[15] S. Kandoi, A. Gokhale, L. Grabow, J. Dumesic, M. Mavrikakis, Catal. Lett. 93 (1/2) (2004) 93.
[16] W. Shan, W. Shen, C. Li, Chem. Mater. 15 (2003) 4761.
[17] Y. Madier, C. Descorme, A.M. Le Govic, D. Duprez, J. Phys. Chem. B 103 (1999) 10999.
[18] W. Liu, M. Flytzani-Stephanopoulos, J. Catal. 153 (1995) 304.
[19] W. Liu, M. Flytzani-Stephanopoulos, J. Catal. 153 (1995) 317.
[20] Y. Liu, Q. Fu, M.F. Stephanopoulos, Catal. Today 93–95 (2004) 246.
[21] J. Xiaoyuan, L. Guanglie, Z. Renxian, M. Jianxin, C. Yu, Z. Xiaoming, Appl. Surf. Sci. 173 (2001) 208.
[22] M. Luo, Y. Zhong, X. Yuan, X. Zheng, Appl. Catal. A: Gen. 162 (1997) 121.
[23] P. Ratnasamy, D. Srinivas, C. Satyanarayana, P. Manikandan, R. Senthil Kumaran, M. Sachin, V. Shetti, J. Catal. 221 (2004) 455.
[24] A. Martinez-Arias, M. Fernández-García, J. Soria, J. Conesa, J. Catal. 182 (1999) 367.
[25] A. Martinez-Arias, M. Fernández-García, O. Gálvez, J. Coronado, J. Anderson, J. Conesa, J. Soria, G. Munuera, J. Catal. 195 (2000) 207.
[26] J. Wang, S. Lin, T. Huang, Appl. Catal. A: Gen. 232 (2002) 107.
[27] G. Jernigan, G. Somorjai, J. Catal. 147 (1994) 567.
[28] S. Kacimi, J. Barbier Jr., R. Taha, D. Duprez, Catal. Lett. 22 (1993) 343.
[29] Lj. Kundakovic, M. Flytzani-Stephanopoulos, Appl. Catal. A: Gen. 171 (1998) 13.
[30] D. Martin, D. Duprez, J. Phys. Chem. 100 (1996) 9429.
[31] D. Martin, Ph.D. Thesis, Poitiers University, 1994.
[32] Th. Osinga, B. Linsen, W. van Beek, J. Catal. 7 (1967) 277.
[33] B. Dvorak, J. Pasek, J. Catal. 18 (1970) 108.
[34] J. Evans, M. Wainwright, A. Bridgwater, D. Young, Appl. Catal. 7 (1983) 75.
[35] Y. Li, Q. Fu, M. Flytzani-Stephanopoulos, Appl. Catal. B: Environ. 27 (2000) 179.
[36] G. Avgouropoulos, T. Ioannides, H. Matralis, J. Batista, S. Hocevar, Catal. Lett. 73 (2001) 33.
[37] G. Avgouropoulos, T. Ioannides, Ch. Papadopoulou, J. Batista, S. Hocevar, H. Matralis, Catal. Today 75 (2002) 157.
[38] G. Sedmak, S. Hocevar, J. Levec, J. Catal. 213 (2003) 135.
[39] P. Mars, D. Van Krevelen, Chem. Eng. Sci. 3 (1954) 41.
[40] S. Bernal, J.J. Calvino, G.A. Cifredo, J.M. Rodriguez-Izquierdo, V. Perrichon, A. Laachir, J. Catal. 137 (1992) 1.
[41] L. Dong, Y. Hu, M. Shen, T. Jin, J. Wang, W. Ding, Y. Chen, Chem. Mater. 13 (2001) 4227.
[42] P. Park, J. Ledford, Catal. Lett. 50 (1998) 41.
[43] T. Huang, D. Tsai, Catal. Lett. 87 (3/4) (2003) 173.
[44] F. Fajardie, J. Tempère, J. Manoli, O. Touret, G. Blanchard, G. Djéga-Mariadassou, J. Catal. 179 (1998) 469.